ApJ, in press
Preprint typeset using LaTeX style emulateapj v. 5/2/11

arXiv:1205.3787v1 [astro-ph.CO] 16 May 2012

IDCS J1426.5+3508: SUNYAEV–ZEL'DOVICH MEASUREMENT OF A MASSIVE IR-SELECTED CLUSTER AT Z = 1.75

M. Brodwin,[1,2] A. H. Gonzalez,[3] S. A. Stanford,[4,5] T. Plagge,[6,7] D. P. Marrone,[8] J. E. Carlstrom[6,7,9] A. Dey,[10] P. R. Eisenhardt,[11] C. Fedeli,[3] D. Gettings,[3] B. T. Jannuzi,[10] M. Joy,[12] E. M. Leitch,[6,7] C. Mancone,[3] G. F. Snyder,[2] D. Stern,[11] and G. Zeimann[4]

ApJ, in press

ABSTRACT

We report 31 GHz CARMA observations of IDCS J1426.5+3508, an infrared-selected galaxy cluster at $z = 1.75$. A Sunyaev–Zel'dovich decrement is detected towards this cluster, indicating a total mass of $M_{200,\mathrm{m}} = (4.3 \pm 1.1) \times 10^{14}\ M_\odot$ in agreement with the approximate X-ray mass of $\sim 5 \times 10^{14} M_\odot$. IDCS J1426.5+3508 is by far the most distant cluster yet detected via the Sunyaev–Zel'dovich effect, and the most massive $z \geq 1.4$ galaxy cluster found to date. Despite the mere $\sim 1\%$ probability of finding it in the 8.82 deg^2 IRAC Distant Cluster Survey, IDCS J1426.5+3508 is not completely unexpected in ΛCDM once the area of large, existing surveys is considered. IDCS J1426.5+3508 is, however, among the rarest, most extreme clusters ever discovered, and indeed is an evolutionary precursor to the most massive known clusters at all redshifts. We discuss how imminent, highly sensitive Sunyaev–Zel'dovich experiments will complement infrared techniques for statistical studies of the formation of the most massive galaxy clusters in the $z > 1.5$ Universe, including potential precursors to IDCS J1426.5+3508.

Subject headings: galaxies: clusters: individual (IDCS J1426.5+3508) — galaxies: clusters: intracluster medium — galaxies: evolution — cosmology: observations — cosmology: cosmic background radiation

1. INTRODUCTION

As the most massive collapsed objects, galaxy clusters provide a sensitive probe of the cosmological parameters that govern the dynamics of the Universe. Traditional cluster cosmology experiments constrain these parameters by comparing predicted cluster mass functions with observed cluster counts (for a review, see Allen et al. 2011).

The recent discovery of a handful of very massive, high redshift ($z > 1$) galaxy clusters (Rosati et al. 2009; Brodwin et al. 2010; Foley et al. 2011) has prompted several studies of the power of individual massive, rare clusters to probe the physics of inflation, in particular non-Gaussianity in the density fluctuations that seed structure formation (Dalal et al. 2008; Brodwin et al. 2010; Holz and Perlmutter 2010; Mortonson et al. 2011; Cayón et al. 2011; Hoyle et al. 2011; Enqvist et al. 2011; Foley et al. 2011; Williamson et al. 2011; Hotchkiss 2011; Paranjape et al. 2011). These rare, massive clusters were all identified from their hot intracluster medium (ICM), whether via X-ray emission or from prominent Sunyaev–Zel'dovich (SZ) decrements.

Conversely, the most successful method for discovering large samples of high redshift galaxy clusters, out to at least $z = 1.5$, is via infrared selection (e.g., Eisenhardt et al. 2008; Muzzin et al. 2008). For instance, the *Spitzer*/IRAC Shallow Cluster Survey (ISCS, Eisenhardt et al. 2008), which employs a full three-dimensional wavelet search technique on a 4.5μm-selected, stellar mass-limited galaxy sample, has discovered 116 candidate galaxy clusters and groups at $z > 1$. More than 20 of these have now been spectroscopically confirmed at $1 < z < 1.5$ (Stanford et al. 2005; Elston et al. 2006; Brodwin et al. 2006; Eisenhardt et al. 2008; Brodwin et al. 2011).

The cosmological importance of individual galaxy clusters depends primarily on their rarity, with the most massive clusters at any redshift providing the most leverage. The maximum predicted cluster mass increases with time due to the growth of structure. Consequently, clusters with moderate masses, by present-day standards, of a few $\times 10^{14}\ M_\odot$ are cosmologically interesting at the highest redshifts (e.g., $z > 1.5$). Only one such cluster, XDCP J0044.0-2033 at $z = 1.58$ (Santos et al. 2011), has been found to date, although at such a high redshift its L_X–based mass is quite uncertain. The most sensitive, large angle, ICM-based cluster survey to date, the 2500 deg^2 South Pole Telescope Survey (SPT; Carlstrom et al. 2011), would only be able to detect such high redshift clusters if they were more massive than

---

[1] Department of Physics and Astronomy, University of Missouri, 5110 Rockhill Road, Kansas City, MO 64110
[2] Harvard-Smithsonian Center for Astrophysics, 60 Garden Street, Cambridge, MA
[3] Department of Astronomy, University of Florida, Gainesville, FL 32611
[4] Department of Physics, University of California, One Shields Avenue, Davis, CA 95616
[5] Institute of Geophysics and Planetary Physics, Lawrence Livermore National Laboratory, Livermore, CA 94550
[6] Kavli Institute for Cosmological Physics, University of Chicago, Chicago, IL 60637
[7] Department of Astronomy and Astrophysics, University of Chicago, Chicago, IL 60637
[8] Steward Observatory, University of Arizona, 933 North Cherry Avenue, Tucson, AZ 85721
[9] Dept. of Physics/Enrico Fermi Institute, University of Chicago, Chicago, IL 60637
[10] NOAO, 950 North Cherry Avenue, Tucson, AZ 85719
[11] Jet Propulsion Laboratory, California Institute of Technology, Pasadena, CA 91109
[12] Department of Space Science, VP62, NASA Marshall Space Flight Center, Huntsville, AL 35812, USA

$\approx 3 \times 10^{14}\, M_\odot$ (Vanderlinde et al. 2010; Andersson et al. 2011). A population of such high-redshift clusters, if massive enough, could provide a powerful opportunity to study the physics of the early Universe and, in particular, to either confirm or falsify the predictions of the ΛCDM paradigm. They would also be invaluable probes of the early formation of massive galaxies in the richest environments.

To extend the ISCS infrared-selected cluster sample to the $z > 1.5$ regime, we carried out the *Spitzer* Deep, Wide–Field Survey (SDWFS, Ashby et al. 2009), which quadrupled the *Spitzer*/IRAC exposure time, leading to a survey more than a factor of 2 deeper than the original IRAC Shallow Survey (Eisenhardt et al. 2004). A new cluster search, the *Spitzer*/IRAC Distant Cluster Survey (IDCS), to be described in detail in forthcoming papers, was carried out using new photometric redshifts calculated for the larger, deeper SDWFS sample. Cluster IDCS J1426.5+3508 at $z = 1.75$ (Stanford et al. 2012, hereafter S12) is the first of the new high–redshift IDCS clusters to be spectroscopically confirmed.

In this paper we report the robust detection of the SZ decrement associated with IDCS J1426.5+3508 in 31 GHz interferometric data taken with the Sunyaev–Zel'dovich Array (SZA), a subarray of the Combined Array for Research in Millimeter-wave Astronomy (CARMA). This is by far the most distant cluster yet detected in the SZ effect, a consequence of the fact that IDCS J1426.5+3508 is the most massive cluster yet discovered at $z > 1.4$. In §2 we briefly describe the discovery of cluster IDCS J1426.5+3508. In §3 we present the CARMA observations and reductions, and describe the measurement of the Comptonization and mass of IDCS J1426.5+3508. We also discuss various systematic uncertainties present in our analysis. In §4, we calculate the likelihood of having found this cluster, given our survey selection function, in a standard ΛCDM cosmology. In §5, we place IDCS J1426.5+3508 in an evolutionary context, finding that it is a precursor to the most massive known clusters at all redshifts. In §6 we discuss our results in light of current and upcoming SZ surveys. We present our conclusions in §7. In this paper, we adopt the WMAP7 cosmology of $(\Omega_\Lambda, \Omega_M, h) = (0.728, 0.272, 0.704)$ of Komatsu et al. (2011). Except where otherwise specified (in §2 and §3.2), we use a cluster mass ($M_{200,\mathrm{m}}$) defined as the mass enclosed within a spherical region of mean overdensity $200 \times \rho_{\mathrm{mean}}$, where ρ_{mean} is the mean matter density on large scales at the redshift of the cluster.

2. CLUSTER IDCS J1426.5+3508

IDCS J1426.5+3508, first reported in S12, was discovered in the IDCS as a striking three-dimensional overdensity of massive galaxies with photometric redshifts at $z_{\mathrm{phot}} \approx 1.8$ (Figure 1, upper right panel). Follow-up spectroscopy, with *HST*/WFC3 in the infrared and Keck/LRIS in the optical, identified seven robust spectroscopic members at $z = 1.75$ and ten additional likely members with less certain redshifts. The *HST* data also revealed the presence of a strong gravitational arc, the analysis and implications of which are discussed in a companion paper (Gonzalez et al. 2012).

IDCS J1426.5+3508 is also detected in shallow *Chandra* data from Murray et al. (2005), with an X-ray luminosity of $L_{0.5\text{-}2\mathrm{keV}} = (5.5 \pm 1.2) \times 10^{44}$ erg/s. Using the M_{500}–L_X scaling relation of Vikhlinin et al. (2009) and the Duffy et al. (2008) mass–concentration relation, this corresponds to a mass of $M_{200,\mathrm{c}} \simeq 5.6 \times 10^{14}\, M_\odot$ (S12)[13]. The *HST*/ACS and WFC3 color image, along with the X-ray detection (yellow contours) are shown in the lower panel of Figure 1.

While IDCS J1426.5+3508 appears from the X-ray data to be impressively massive, particularly at such an extreme redshift, the X-ray luminosity is based on only 54 cluster X-ray photons. Further, it relies on a high-scatter mass proxy, the $M_{500,\mathrm{c}}$-L_X relation, which is only calibrated at low ($z < 1$) redshift. The uncertainty of this X-ray mass estimate is at least $\sim 40\%$.

3. DATA

3.1. *Sunyaev Zel'dovich Observations*

IDCS J1426.5+3508 was observed with the SZA, an 8-element radio interferometer optimized for measurements of the SZ effect. During the time in which the data were obtained, the array was sited at the Cedar Flat location described in Culverhouse et al. (2010), and was in the "SL" configuration. In this configuration, six elements comprise a compact array sensitive to arcminute-scale SZ signals, and two outrigger elements provide simultaneous discrimination for compact radio source emission. The compact array and outrigger baselines provide baseline lengths of 0.35-1.3 kλ and 2-7.5 kλ, respectively.

The cluster was observed for four sidereal passes on nights ranging over UT 2011 June 9–29, for a total of 6.24 hours of unflagged, on-source integration time. Data were obtained in an 8 GHz passband centered at 31 GHz. The resulting noise level achieved by the short (SZ-sensitive) baselines was 0.29 mJy/beam, or 22 $\mu\mathrm{K}_{\mathrm{RJ}}$ with a synthesized beam of $118'' \times 143''$. For the long baselines, the noise level achieved was 0.29 mJy/beam in a $19\farcs9 \times 14\farcs4$ beam. The data were reduced using the Miriad software package (Sault et al. 1995), and the absolute calibration was determined using periodic measurements of Mars calibrated against the Rudy et al. (1987) model. A systematic uncertainty of 5% has been applied to the SZ measurements due to the uncertainty in the absolute calibration. The SZA map is shown in the upper left panel of Figure 1.

3.2. *Comptonization and Mass of IDCS J1426.5+3508*

To determine the properties of IDCS J1426.5+3508 from the SZA data, we make use of the fact that the integrated Compton y-parameter scales with total mass. Assuming a spherically symmetric pressure distribution within the cluster, the integrated y-parameter is given by

$$Y D_A^2 = \frac{\sigma_T}{m_e c^2} \int P(r) dV, \tag{1}$$

where D_A is the angular diameter distance, σ_T is the Thomson cross-section of an electron, m_e is the electron mass, c is the speed of light, $P(r)$ is the pressure profile, and the integral is over a spherical volume centered on the cluster (see, e.g., Marrone et al. 2011). The pressure

---

[13] In S12 the mass is measured with respect to a critical overdensity, rather than mean overdensity we use in this paper.

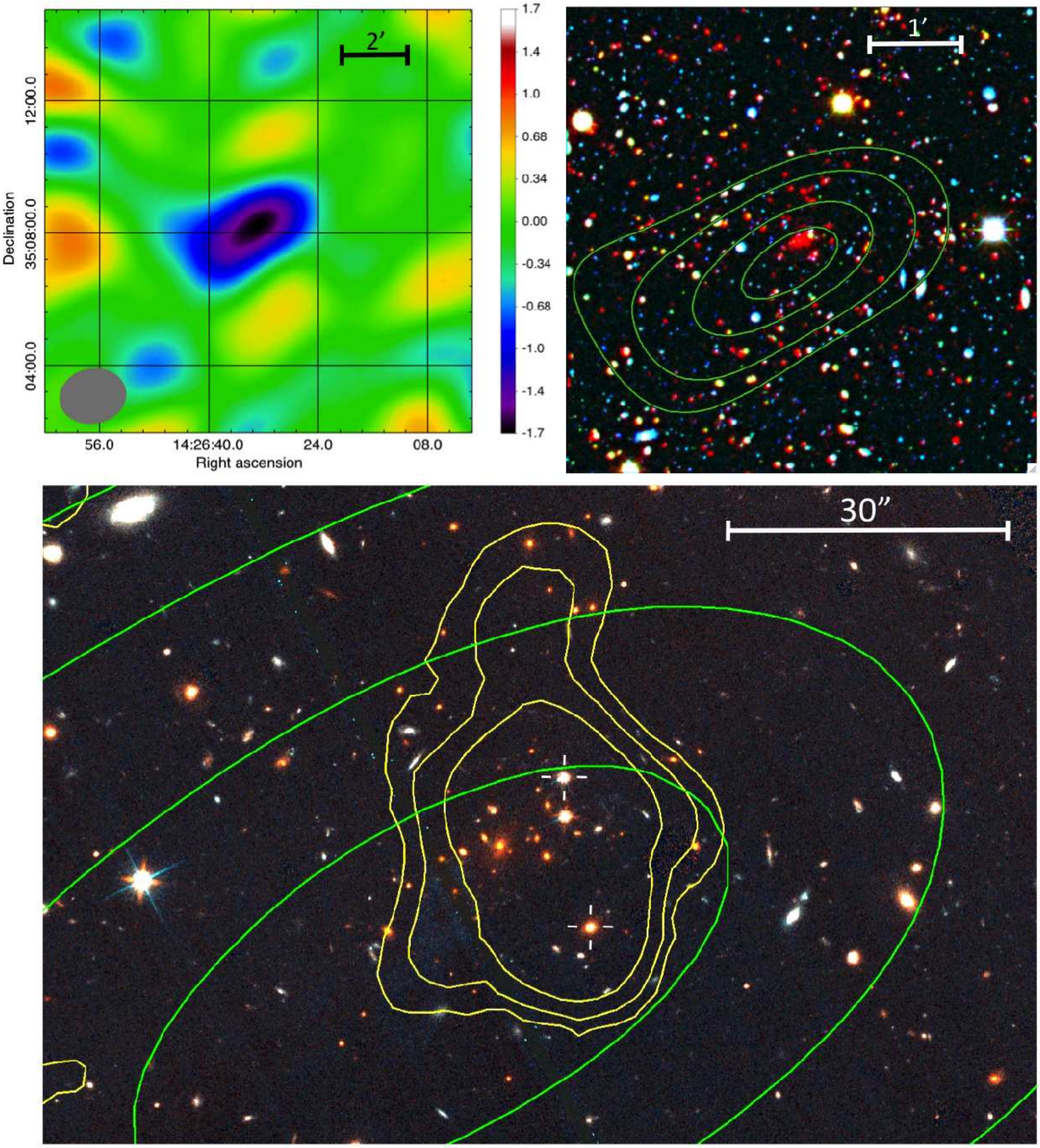

Figure 1. *Upper left:* $12.8' \times 12.8'$ SZA mm-wave map showing the SZ decrement of IDCS J1426.5+3508. The flux scale in mJy/beam is shown to the right of the map, and the FWHM of the CLEAN beam is shown in the lower left corner. *Upper right:* A $5'$ $\times$ $5'$ $B_W R[4.5]$ pseudo-color image of IDCS J1426.5+3508, with the SZ contours overplotted. The optical and infrared data are from the NOAO Deep, Wide–Field Survey (NDWFS; Jannuzi and Dey 1999) and SDWFS, respectively. *Lower panel: HST* F814W+F160W pseudo-color zoom–in of IDCS J1426.5+3508. The SZ contours (green) from the present work and X-ray contours (yellow) from S12, corresponding to 0.131, 0.077 and 0.044 counts per $2'' \times 2''$ pixel in 8.3 ks in the 0.5-2 KeV band, are overplotted. Two sources are indicated by hash marks. The northern source is an X-ray luminous QSO that is also a cluster member; the southern source is a radio-bright AGN, the emission from which was removed from the SZA map. Both are discussed further in the text. In all panels North is up, East is left, and a scale bar is given.

profile $P(r)$ is determined by fitting a model profile to the SZA data. We adopt the generalized Navarro et al. (1997) model proposed by Nagai et al. (2007):

$$P(r) = \frac{P_0}{x^{\gamma}(1+x^{\alpha})^{(\beta-\gamma)/\alpha}}, \tag{2}$$

where $x = r/r_s$. We fix the power law exponents (α, β, γ) to the "universal" values reported by Arnaud et al. (2010), and leave P_0 and r_s free to vary[14].

One important source of systematic errors in SZ cluster measurements is radio point sources. These synchrotron sources are often variable, are known to be correlated with clusters, and can fill in the SZ decrement at low frequencies (see, e.g., Carlstrom et al. 2002). Wide angular scale surveys such as the SPT survey generally mask regions where bright point sources are detected, which changes the survey selection function but can be accounted for using simulations (Vanderlinde et al. 2010). However, for targeted SZ follow-up of sources selected in other bands, point source fluxes must be measured and removed in order to accurately estimate the cluster mass. Due to the temporal variability of these sources, the point source fluxes ideally should be determined concurrently with the SZ measurement. The SZA uses its longer outrigger baselines to perform such simultaneous point source measurements. For spatially compact sources, the emission measured on the outrigger baselines (smaller angular scales) can be assumed to be representative of the emission measured on the short SZ-sensitive baselines (larger angular scales), and can thereby be removed from the SZ signal (see, e.g., Muchovej et al. 2007).

Two such point sources were discussed in S12 and are indicated by hash marks in Figure 1. The northern source is an X-ray bright QSO that is also a spectroscopically confirmed member of IDCS J1426.5+3508. As described in S12, the contribution to the cluster's X-ray flux from this QSO had to be removed to obtain a reliable cluster mass. This QSO is not detected in the radio, however, with a formal 31 GHz flux density of -0.04 ± 0.31 mJy, and therefore it has no impact on the measured cluster mass. A second point source, bright enough in the radio to fill in the SZ decrement of IDCS J1426.5+3508, was identified near the cluster center at $14^{\mathrm{h}}26^{\mathrm{m}}32\overset{\mathrm{s}}{.}1$, $35^{\circ}08'15\overset{''}{.}2$, indicated by the southern hash mark in Figure 1. This source corresponds to a ~ 95 mJy source identified at 1.4 GHz in the NVSS (Condon et al. 1998) and FIRST (Becker et al. 1995) catalogs. The lower–frequency radio survey data indicate that this source is unresolved at the angular scales to which the SZA is sensitive, allowing it to be modeled as a point source and constrained using the long baseline data. The flux density of this source is left as a free parameter in the cluster model fit, and is found to be 5.3 ± 0.3 mJy. The resulting spectral index of -0.93 ± 0.02 is consistent with synchrotron radiation.

A Markov Chain Monte Carlo (MCMC) fit is used to jointly constrain P_0, r_s, and the flux densities of the two point sources in our fiducial cosmology. The results of this fit are used to compute the integrated y-parameter and the total cluster mass. By convention, both the total cluster mass and the integrated y-parameter are reported within a radius corresponding to a fixed overdensity $\Delta = 500$ relative to the critical density of the Universe at the redshift of the cluster. The integrated quantities are determined by finding the overdensity radius r_{500} (equivalent to the mass, since $M_{\Delta} = (4\pi r_{\Delta}^3/3)\Delta\rho_c(z)$) and integrated y-parameter Y_{500} that are mutually consistent with the Andersson et al. (2011) M_{500}–Y_{500} scaling relation. We choose this relation since the clusters with which it is measured have the highest mean redshift. The self-consistent values of r_{500} and Y_{500} are determined iteratively at each step in the MCMC, and the scaling relation parameters are sampled at each step using their reported means and variances. Using this method, we find that $M_{500,\mathrm{c}} = (2.6 \pm 0.7) \times 10^{14}$ $M_{\odot}$, where the error is statistical in nature. Assuming the Duffy et al. (2008) concentration relation, this corresponds to $M_{200,\mathrm{c}} = (4.1 \pm 1.1) \times 10^{14}$ $M_{\odot}$. This mass agrees well with the X-ray mass of $M_{200,\mathrm{c}} \simeq 5.6 \times 10^{14}$ $M_{\odot}$, for which the error is at least 40%.

A significant uncertainty, inherent to both SZ and X-ray measurements of the masses of high redshift clusters, is due to the fact that no published mass-observable scaling relation has been estimated using a sample containing clusters at redshifts significantly greater than unity. While Andersson et al. (2011) found no compelling evidence for redshift evolution in the M_{500}–Y_{500} scaling relation out to $z \sim 1$, their sample consisted of lower-redshift and higher-mass objects whose scaling properties may be systematically different from those of IDCS J1426.5+3508.

To enable the SZ mass of IDCS J1426.5+3508 to be easily calculated with future scaling relations, we also report the spherically-averaged dimensionless Comptonization, $Y_{\mathrm{sph},500} = (7.9 \pm 3.2) \times 10^{-12}$. This corresponds to a gas mass at r_{500} of $M_{\mathrm{gas}} = (2.9 \pm 1.2) \times 10^{13}$ $M_{\odot}$ for a constant temperature of 5 keV. This temperature is consistent with the X-ray measurement (S12); for a cooler 4 keV cluster the inferred gas mass would increase by 25%.

To assess the SZ detection significance, we fit a cluster model to the visibility data and compare to a null model. Our model consists of an elliptical Gaussian SZ decrement located at the X-ray centroid along with the nearby radio point source, and our null model consists only of the point source. We find a $\Delta\chi^2$ of 37.65 between the model and null model fits. Since the (fixed-position) elliptical Gaussian adds four degrees of freedom, this $\Delta\chi^2$ corresponds to a detection significance of 5.3 σ, or a false detection probability of 1.32×10^{-7}. Because the SZ signal was sought only at the position of the X-ray emission, this detection is very secure. In contrast, a false 5.3 sigma detection is far more plausible in a wide–field survey like SPT because there are of order 10^6 independent pixels in which such a deviation can arise by chance. We therefore consider the pointed, follow-up detection of IDCS J1426.5+3508 to be robust.

If the cluster position is not fixed to the X-ray centroid, the best–fit centroid of the SZ signal is $14^{\mathrm{h}}26^{\mathrm{m}}34\overset{\mathrm{s}}{.}0$, $35^{\circ}08'02\overset{''}{.}6$, which is slightly offset ($\approx 32''$ and $25''$) from the X-ray and BCG positions, respectively. As the uncertainty in the SZ centroid is $\approx 35''$, this offset is not statistically significant. Absent the X-ray positional prior, the significance of the SZ detection is almost identical (5.2 σ).

---

[14] Arnaud et al. (2010) suggest other power law exponents appropriate for clusters with a known morphology, but Marrone et al. (2011) find that these alternative choices make a $\lesssim 5\%$ difference in the estimate of Y_{500}.

4. PROBABILITY OF EXISTENCE IN A ΛCDM UNIVERSE

While not as massive as the $z \sim 1$ SPT clusters, IDCS J1426.5+3508, by virtue of its exceptional redshift and substantial mass, is arguably one of the more extreme systems discovered to date. It is therefore interesting to calculate the probability of discovering it in the IDCS in a standard ΛCDM Universe.

We use the exclusion curve formalism presented in Mortonson et al. (2011, hereafter M11), which tests whether a single cluster is rare enough to falsify ΛCDM and quintessence at a given significance level, accounting for both sample and parameter variance. The M11 formalism uses cluster masses measured within a sphere defined by an overdensity 200 times the mean, rather than critical, density of the Universe. In this convention, adopting the Duffy et al. (2008) mass–concentration relation, IDCS J1426.5+3508 has a mass of $M_{200,\rm m} = (4.3 \pm 1.1) \times 10^{14}\ M_\odot$.

The M11 formalism requires that observed cluster masses be corrected for Eddington bias caused by the steep slope of the cluster mass function at this mass scale and redshift. We follow the prescription given in Appendix A of M11:

$$\ln M = \ln M_{\rm obs} + \frac{1}{2}\gamma\sigma^2_{\ln M}, \qquad (3)$$

where M is the expected value for the true mass given the observed mass, γ is the local slope of the mass function, and σ is the uncertainty associated with the observations. Here we use the fitting function for γ provided in M11, which yields $\gamma = -5.8$. We thus derive that the expected value for this bias-corrected mass is $M_{200,\rm m} = (3.6 \pm 0.9) \times 10^{14}\ M_\odot$.

In Figure 2 we plot the appropriately bias-corrected mass for IDCS J1426.5+3508 along with 95% confidence exclusion curves using the M11 prescription. For comparison we include rare, massive clusters from the SPT survey (Williamson et al. 2011; Brodwin et al. 2010) and other massive $z > 1$ clusters from the ISCS for which weak lensing or X-ray masses are available (Brodwin et al. 2011; Jee et al. 2011). All masses are deboosted in accordance with the M11 prescription.

The lowest curve in the figure corresponds to the 95% exclusion curve for clusters within the 8.82 deg^2 IDCS area. The central value of the deboosted SZ mass is above the curve, formally falsifying ΛCDM at the 95% level. We note, however, that the statistical error bar overlaps the exclusion curve. Furthermore, uncertainties in the scaling relation could easily lower the mass below the exclusion curve.

Rather than asking whether such a cluster should have been detected in the IDCS, perhaps a fairer question is to ask whether such a cluster should have been detected in the full area of sky covered by all cluster surveys capable of detecting such a cluster. Numerous X-ray surveys of varying areas and depths could have detected IDCS J1426.5+3508, but for simplicity we consider the SPT survey, which has the sensitivity to detect clusters like IDCS J1426.5+3508, even at $z = 1.75$ (Vanderlinde et al. 2010). The first 178 deg^2 of the SPT survey does not contain a single cluster comparable to IDCS J1426.5+3508 in mass and redshift (Vanderlinde et al. 2010), which suggests that the true abundance of such clusters is far lower than our discovery would indicate. Neither the Atacama Cosmology Telescope (ACT) project nor the *Planck* project surveys are sensitive enough to detect IDCS J1426.5+3508 (Marriage et al. 2011; Planck Collaboration et al. 2011). If we consider IDCS J1426.5+3508 to have been drawn from an area of at least ~ 178 deg^2 (shown as the cyan curve in Fig. 2) rather than the IDCS volume, then the cluster is no longer in contradiction with ΛCDM; we were simply somewhat lucky to detect it in the comparatively tiny (8.82 deg^2) IDCS area.

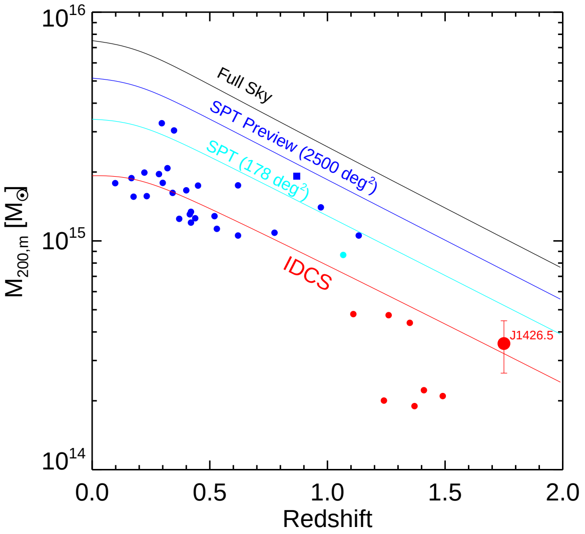

Figure 2. M11-style plot showing the mass and redshift of IDCS J1426.5+3508 (large red circle), along with other $z > 1$ ISCS clusters (Brodwin et al. 2011; Jee et al. 2011, small red circles) and SPT clusters (Williamson et al. 2011, small blue circles; Brodwin et al. 2010, small cyan circle). The solid red curve is the 95% exclusion curve for the IDCS area. The cyan, blue and black curves are the exclusion curves for the currently published full depth SPT survey (178 deg^2, Vanderlinde et al. 2010), the 2500 deg^2 SPT preview survey of Williamson et al. (2011) and the full sky, respectively. The square symbol represents cluster SPT-CL J0102-4915, first reported as ACT-CL J0102-4915 (Menanteau et al. 2010). We plot this cluster at the spectroscopic redshift of $z = 0.870$ reported in Menanteau et al. (2012). All clusters are color-coded to the appropriate exclusion curve.

5. EVOLUTION TO THE PRESENT DAY

Although the mere existence of IDCS J1426.5+3508 may not have significant cosmological implications, it is nevertheless among the rarest, most extreme clusters ever discovered. As such, it is interesting to understand its nature in the context of the growth of the largest structures.

Using the Tinker et al. (2008) mass function, we first identify the space density of clusters at $z = 1.75$ that have masses greater to or equal to that of IDCS J1426.5+3508. At each redshift we then associate the clusters with that space density with its descendents. In Figure 3 we plot the mass evolution of IDCS J1426.5+3508 (large red circle) from $z = 1.75$ to the present day (thick black line). For comparison we also plot a representative selection of the most extreme clusters found to date at all redshifts. This abundance–matching calculation is designed to predict the mean expected growth of IDCS J1426.5+3508. We note that there are intrinsic variations in accretion histories due to the stochastic nature of mergers (e.g., Wechsler et al. 2002), but consider a full treatment beyond the scope of the present work.

As demonstrated in this figure, IDCS J1426.5+3508 is much more than just another massive, very high redshift cluster. It is an evolutionary precursor to the most massive known clusters at all redshifts. Indeed, its descendent population consists of the most massive virialized objects ever discovered.

There are no other confirmed clusters at $z > 1.75$ with masses greater than $10^{14}\ M_\odot$. Between $1.5 < z < 1.75$ only one cluster, XDCP J0044.0-2033 at $z = 1.58$ (Santos et al. 2011; Fassbender et al. 2011), is comparable to IDCS J1426.5+3508, though it is somewhat less massive and below the growth trend.

The most massive $z > 1$ X-ray selected cluster, XMMU J2235.3-2557 at $z = 1.39$ (Mullis et al. 2005; Rosati et al. 2009), falls along the evolutionary path of IDCS J1426.5+3508, as does the most massive $z > 1$ cluster in the SPT survey, SPT-CL 2106-5844 at $z = 1.13$ (Foley et al. 2011; Williamson et al. 2011). Similarly, the only $z \sim 1$ *Planck* cluster reported to date, PLCK G266.6-27.3 at $z = 0.94$ is also consistent.

SPT-CL J0102-4915, first reported as ACT-CL J0102-4915 from the ACT survey (Menanteau et al. 2010; Marriage et al. 2011), is among the most significant detections overall in both of these SZ surveys. Masses of this cluster from the two SZ surveys are plotted as the square symbols at the spectroscopic redshift of $z = 0.870$ (Menanteau et al. 2012). The lower SPT mass is measured from the SZ decrement, whereas the higher ACT mass (slightly offset in redshift for clarity) is combined from several methods. The masses are consistent within the errors. IDCS J1426.5+3508 is consistent with growing into a cluster like this as well. RX J1347-1145 (Allen et al. 2002; Lu et al. 2010) is the most luminous X-ray cluster in the sky, though it is not quite massive enough to be considered a descendent of IDCS J1426.5+3508. In the local Universe the Coma cluster represents the kind of extreme cluster IDCS J1426.5+3508 will evolve into.

Holz and Perlmutter (2010) recently predicted the properties of the single most massive cluster that can form in a ΛCDM Universe with Gaussian initial conditions and where the growth of structure follows the predictions of general relativity. They predict this cluster should be found at $z = 0.22$ and have a mass of $M_{200,\mathrm{m}} = 3.8 \times 10^{15}\ M_\odot$. Their 68% contour in predicted mass and redshift is shown as a light blue contour and labeled HP10 in the figure. IDCS J1426.5+3508 is completely consistent with being an evolutionary precursor to the most massive halo predicted to exist in the observable Universe.

6. DISCUSSION

Given its extreme mass it is not surprising that IDCS J1426.5+3508 was detected in shallow (5 ks) *Chandra* images (S12), despite its high redshift. The robust, high-significance SZA detection reported herein confirms that IDCS J1426.5+3508 is one of the most massive collapsed structures evolving in the Universe. Although it was discovered in a small (≈ 9 deg^2) infrared-selected cluster survey, the odds of finding such a rare, massive cluster were quite low, 0.8% (0.2%) using the Holz and Perlmutter (2010) formalism with the deboosted (measured) mass. Finding the precursors of IDCS J1426.5+3508 at even earlier times will require much larger surveys.

In this section we examine why the current generation of SZ surveys, despite covering areas ranging from 10^2–10^4 deg^2, have not yet seen a cluster as extreme as IDCS J1426.5+3508 at $z > 1.5$. We also discuss the potential of the next generation of SZ surveys to discover its evolutionary precursors.

6.1. *Current SZ surveys*

The detectability of a cluster like IDCS J1426.5+3508 in an SZ cluster survey depends on three factors. The survey must have sufficient mass sensitivity at high redshift, it must cover sufficient area so that the expectation value of the number of clusters is greater than unity, and the clusters in question must not contain bright radio point sources nor have any along the line of sight.

In terms of sensitivity, only the SPT survey is currently capable of detecting IDCS J1426.5+3508 at this high redshift. Vanderlinde et al. (2010) report a formal 50% completeness of $M_{200,\mathrm{m}} \approx 3.5 \times 10^{14}\ M_\odot$ at $z = 1.5$, and this improves to $\gtrsim 90\%$ at $z = 1.75$. That mass limit is below both the measured and deboosted mass of IDCS J1426.5+3508. So the SPT should nominally have detected such a cluster were it present at $z = 1.75$ in the single-band analysis of their first 178 deg^2 (Vanderlinde et al. 2010). However, since the SPT completeness limit at high redshift is uncertain at the 30% level in mass (Vanderlinde et al. 2010), the non-detection of a single high–redshift cluster like IDCS J1426.5+3508 is unremarkable.

A more interesting question, related to the second criterion and to the rarity analysis of §4, is that of how many such clusters are actually expected in the current SPT area? According to the Holz and Perlmutter (2010) formulation, we expect only 0.2 such clusters in 178 deg^2, and therefore none should have been found. In the complete, full-depth 2500 deg^2 SPT survey, Holz and Perlmutter (2010) predict the presence of 2.4 such clusters, though shot noise will play a role in whether any are found.

Finally, as discussed in §3.2, IDCS J1426.5+3508 has a radio–bright AGN at $z = 1.535$ along the line-of-sight, indicated by the southern hash marks in Figure 1. At a redshift separation of $\Delta z > 0.2$, it is not physically associated with the cluster. Its radio emission was constrained using the long SZA baselines, which are insensitive to the arcminute angular scale SZ decrement. If the measured 1.4 to 31 GHz spectral index of this source (-0.93) is valid to 150 GHz, the AGN flux would be 1.2 mJy at this frequency, well below the 5 mJy threshold for masking individual point sources in the SPT survey. However, it would partially fill in the ~ 14 mJy SZ decrement at 150 GHz, reducing the SPT detection significance and biasing the mass estimate low by $\sim 10 - 15\%$.

It is possible that the AGN content of clusters at the highest redshifts may be substantially larger than at in-

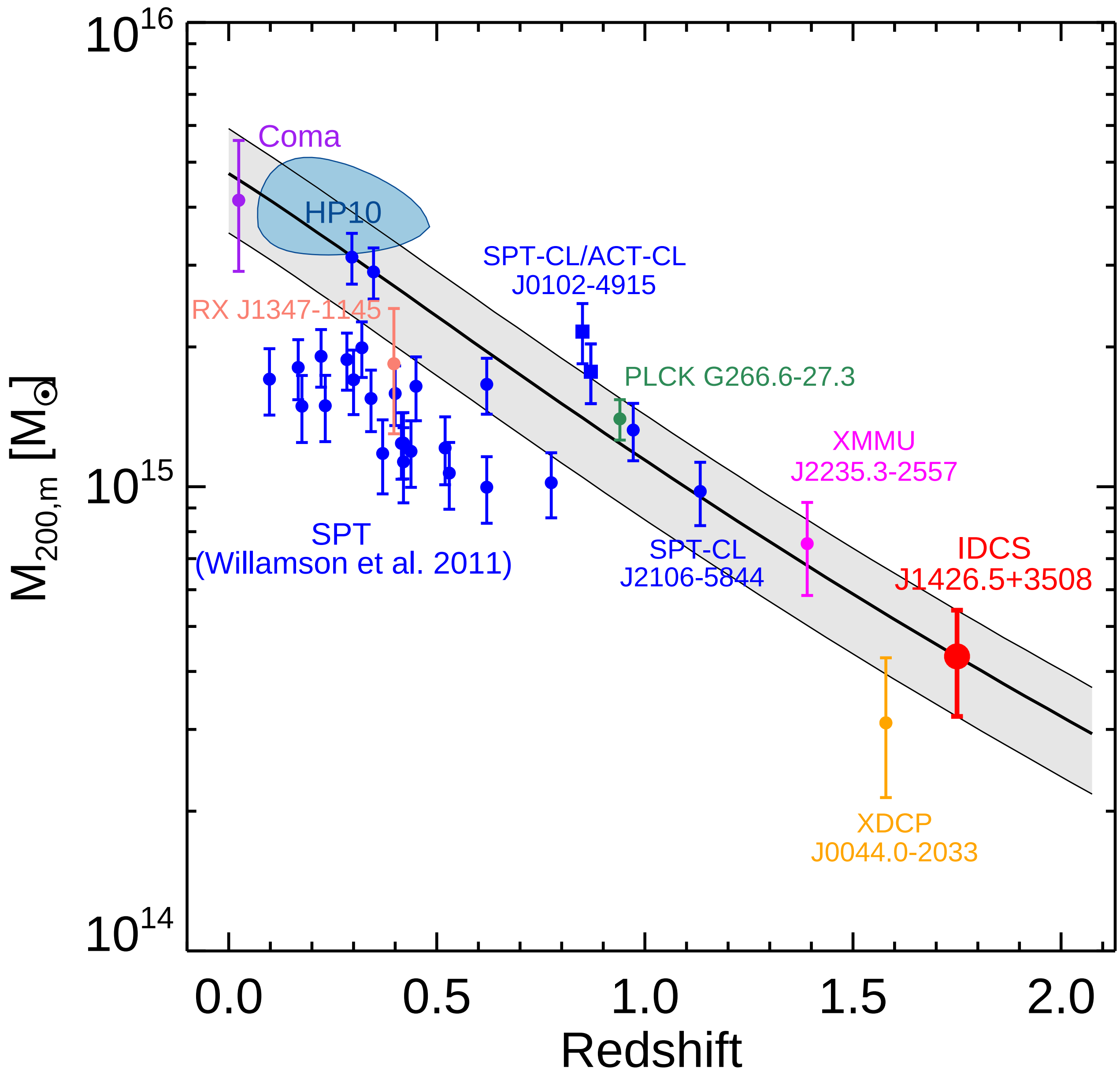

Figure 3. Predicted mass growth of IDCS J1426.5+3508 vs. redshift based on abundance matching. IDCS J1426.5+3508 is the large red circle and the predicted growth in its mass is shown as a thick black line. The 1 σ errors, stemming from the mass measurement errors, are shown as the shaded region. An assortment of the rarest, most massive clusters found at all redshift is shown for comparison and discussed in the text. SPT-CL J0102-4915 was first reported as ACT-CL J0102-4915 by Menanteau et al. (2010) and Marriage et al. (2011). The independent mass measurements from both surveys are plotted as the square symbols for this cluster at the spectroscopic redshift ($z = 0.8701$) reported in Menanteau et al. (2012). IDCS J1426.5+3508 is consistent with being a member of the most extreme population of virialized structures in the Universe.

termediate ($z < 1$) redshifts. Indeed, Galametz et al. (2009) find evidence for a strong increase in the incidence of AGN in clusters with redshift from $0.2 < z < 1.4$, particularly for X-ray and IR-selected AGN. The evidence for rapid number density evolution in radio-selected AGN is not as conclusive. In some surveys (e.g., Galametz et al. 2009) it increases as quickly in clusters as in the field, whereas others (e.g., Gralla et al. 2011) find it is roughly constant. One major advantage of CARMA for targeted SZ observations of clusters is the ability to simultaneously identify and remove contamination from such (generally variable) sources, as in this work, and thus recover accurate cluster masses.

6.2. *Next–Generation SZ surveys*

Several next–generation SZ experiments designed for CMB polarization measurements, such as SPTpol (Bleem et al. 2012) and ACTpol (Niemack et al. 2010), are currently being deployed. These experiments will possess typical SZ mass sensitivities a factor of several lower than present surveys. Here we calculate the expected yield of high–redshift clusters similar to IDCS J1426.5+3508 for a canonical 500 deg^2 next–generation survey with constant $M_{200,\mathrm{m}}$ completeness limits of 1.2×10^{14} $M_\odot$ and 1.5×10^{14} $M_\odot$ at the 50% and 90% levels, respectively.

The same methodology that explains the lack of a cluster like IDCS J1426.5+3508 in the current SPT survey area predicts that a significant number of very high redshift clusters, somewhat less massive than IDCS J1426.5+3508, will be found with the polarization experiments. Figure 4 shows the expected cumulative yield, based on the Holz and Perlmutter (2010) formulation, at the two mass limits given above, accounting for the expected completenesses.

The combination of area and depth of the next generation SZ surveys will allow them to identify a large statistical sample of massive, hot clusters at $1.5 < z < 2.0$. As such they provide a natural extension of the infrared surveys, which have characterized galaxy clusters to $z = 1.5$. A 100 deg^2 region that will be covered by both SPTpol and ACTpol will also contain *Spitzer* infrared data, from an ongoing *Spitzer* Exploration Class program (PID 80096, PI Stanford). This will allow optimal high-redshift cluster detection and study at both IR and mm wavelengths, the only two cluster probes that are nearly redshift-independent at $1 < z < 2$.

Despite the wealth of new, high redshift clusters to be found by the next-generation SZ surveys, there are only even odds ($p \sim 0.5$) of finding a $z = 2$ precursor to IDCS J1426.5+3508. Unless, of course, we are fortunate once again.

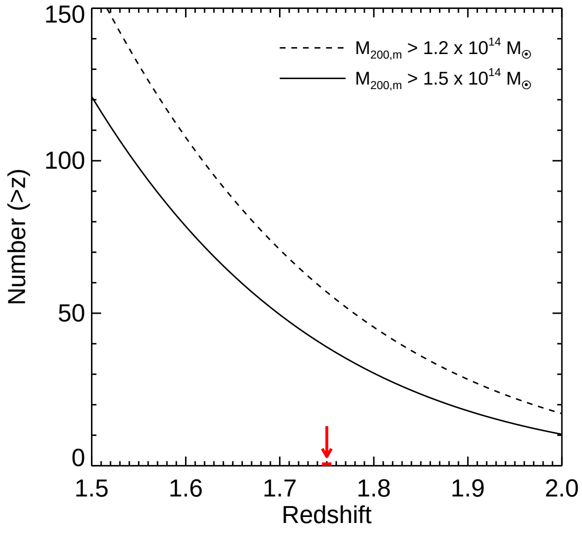

Figure 4. Predicted cumulative counts of massive $1.5 < z < 2$ clusters at the 50% ($M_{200,\mathrm{m}} = 1.20 \times 10^{14}$ $M_\odot$) and 90% ($M_{200,\mathrm{m}} = 1.5 \times 10^{14}$ $M_\odot$) completeness limits of a representative 500 deg^2 next–generation SZ survey. The curves account for losses due to incompleteness. The arrow indicates the redshift of IDCS J1426.5+3508.

7. CONCLUSIONS

We have presented a robust 5.3 σ SZ detection of the infrared-selected cluster IDCS J1426.5+3508 at $z = 1.75$, by far the most distant cluster with an SZ detection to date. Using the Andersson et al. (2011) M_{500}–Y_{500} scaling relation, we find $M_{200,\mathrm{m}} = (4.3 \pm 1.1) \times 10^{14}$ $M_\odot$, in agreement with the X-ray mass reported in S12.

The chance of finding IDCS J1426.5+3508 in the ∼ 9 deg^2 IDCS was $\lesssim$ 1%, which, taken at face value, marginally rules out ΛCDM. Within the much larger total area probed by other SZ and X-ray surveys, its existence is not unexpected.

In a ΛCDM cosmology, with the growth of structure as predicted by general relativity, IDCS J1426.5+3508 will grow to a mass of $M_{200,\mathrm{m}} \approx 4.7 \times 10^{15}$ $M_\odot$ by the present day. It therefore shares an evolutionary path with the most massive known clusters at every redshift. Along with several of the rarest, high-redshift clusters currently known, IDCS J1426.5+3508 is consistent with evolving into the single most massive cluster expected to exist in the observable Universe.

Support for CARMA construction was derived from the states of California, Illinois, and Maryland, the James S. McDonnell Foundation, the Gordon and Betty Moore Foundation, the Kenneth T. and Eileen L. Norris Foundation, the University of Chicago, the Associates of the California Institute of Technology, and the National Science Foundation. Ongoing CARMA development and operations are supported by the National Science Foundation under a cooperative agreement, and by the CARMA partner universities. The work at Chicago is supported by NSF grant AST-0838187 and PHY-0114422.

This work is based in part on observations made with the *Spitzer Space Telescope*, which is operated by the Jet Propulsion Laboratory, California Institute of Technology under a contract with NASA. Support for this work was provided by NASA through an award issued by JPL/Caltech. This work is based in part on observations obtained with the *Chandra X-ray Observatory* (CXO), under contract SV4-74018, A31 with the Smithsonian Astrophysical Observatory which operates the CXO for NASA. Support for this research was provided by NASA grant G09-0150A. Support for *HST* programs 11663 and 12203 were provided by NASA through a grant from the Space Telescope Science Institute, which is operated by the Association of Universities for Research in Astronomy, Inc., under NASA contract NAS 5-26555. This work is based in part on data obtained at the W. M. Keck Observatory, which is operated as a scientific partnership among the California Institute of Technology, the University of California and the National Aeronautics and Space Administration. The Observatory was made possible by the generous financial support of the W. M. Keck Foundation. This work makes use of image data from the NOAO Deep Wide–Field Survey (NDWFS) as distributed by the NOAO Science Archive. NOAO is operated by the Association of Universities for Research in Astronomy (AURA), Inc., under a cooperative agreement with the National Science Foundation.

We thank the anonymous referee for suggestions which improved the manuscript, Bradford Benson for helpful discussions, F. Will High and Keith Vanderlinde for providing published SPT masses in a digital form, Matt Ashby for creating the IRAC catalogs for SDWFS, Michael Brown for combining the NDWFS with SDWFS catalogs, Alexey Vikhlinin for advice on the analysis of the *Chandra* data, and Daniel Holz for providing his predictions in an electronic format. This paper would not have been possible without the efforts of the support staffs of CARMA, the Keck Observatory, *Spitzer Space Telescope*, *Hubble Space Telescope*, and *Chandra X-ray Observatory*. Support for MB was provided by the W. M. Keck Foundation. AHG acknowledges support from the National Science Foundation through grant AST-0708490. The work by SAS at LLNL was performed under the auspices of the U. S. Department of Energy under Contract No. W-7405-ENG-48.

REFERENCES

Allen, S. W., Evrard, A. E., and Mantz, A. B. 2011, *ARA&A,* submitted (arXiv:1103.4829)

Allen, S. W., Schmidt, R. W., and Fabian, A. C. 2002, *MNRAS,* **335**, 256

Andersson, K., et al. 2011, *ApJ,* **738**, 48

Arnaud, M., Pratt, G. W., Piffaretti, R., Böhringer, H., Croston, J. H., and Pointecouteau, E. 2010, *A&A,* **517**, A92

Ashby, M. L. N., et al. 2009, *ApJ,* **701**, 428

Becker, R. H., White, R. L., and Helfand, D. J. 1995, *ApJ,* **450**, 559

Bleem, L., et al. 2012, *Journal of Low Temperature Physics* pp 1–6, 10.1007/s10909-012-0505-y

Brodwin, M., et al. 2006, *ApJ,* **651**, 791

Brodwin, M., et al. 2010, *ApJ,* **721**, 90

Brodwin, M., et al. 2011, *ApJ,* **732**, 33

Carlstrom, J. E., et al. 2011, *PASP,* **123**, 568

Carlstrom, J. E., Holder, G. P., and Reese, E. D. 2002, *ARA&A,* **40**, 643

Cayón, L., Gordon, C., and Silk, J. 2011, *MNRAS,* **415**, 849

Condon, J. J., Cotton, W. D., Greisen, E. W., Yin, Q. F., Perley, R. A., Taylor, G. B., and Broderick, J. J. 1998, *AJ,* **115**, 1693

Culverhouse, T. L., et al. 2010, *ApJ,* **723**, L78

Dalal, N., Doré, O., Huterer, D., and Shirokov, A. 2008, *Phys. Rev. D,* **77**, 123514

Duffy, A. R., Schaye, J., Kay, S. T., and Dalla Vecchia, C. 2008, *MNRAS,* **390**, L64

Eisenhardt, P. R., et al. 2004, *ApJS,* **154**, 48

Eisenhardt, P. R. M., et al. 2008, *ApJ,* **684**, 905

Elston, R. J., et al. 2006, *ApJ,* **639**, 816

Enqvist, K., Hotchkiss, S., and Taanila, O. 2011, *J. Cosmology Astropart. Phys.,* **4**, 17

Fassbender, R., et al. 2011, *New Journal of Physics,* in press (arXiv:1111.0009)

Foley, R. J., et al. 2011, *ApJ,* **731**, 86

Galametz, A., et al. 2009, *ApJ,* **694**, 1309

Gonzalez, A. H., et al. 2012, *ApJ,* submitted

Gralla, M. B., Gladders, M. D., Yee, H. K. C., and Barrientos, L. F. 2011, *ApJ,* **734**, 103

Holz, D. E. and Perlmutter, S. 2010, arXiv:1004.5349

Hotchkiss, S. 2011, *J. Cosmology Astropart. Phys.,* **7**, 4

Hoyle, B., Jimenez, R., and Verde, L. 2011, *Phys. Rev. D,* **83(10)**, 103502

Jannuzi, B. T. and Dey, A. 1999, in *ASP Conf. Ser. 191 — Photometric Redshifts and the Detection of High Redshift Galaxies*, p. 111

Jee, M. J., et al. 2011, *ApJ,* **737**, 59

Komatsu, E., et al. 2011, *ApJS,* **192**, 18

Lu, T., et al. 2010, *MNRAS,* **403**, 1787

Marriage, T. A., et al. 2011, *ApJ,* **737**, 61

Marrone, D. P., et al. 2011, *ApJ,* submitted (arXiv:1107.5115)

Menanteau, F., et al. 2010, *ApJ,* **723**, 1523

Menanteau, F., et al. 2012, *ApJ,* in press (arXiv:1109.0953)

Mortonson, M. J., Hu, W., and Huterer, D. 2011, *Phys. Rev. D,* 83(2)

Muchovej, S., et al. 2007, *ApJ,* **663**, 708

Mullis, C. R., Rosati, P., Lamer, G., Böhringer, H., Schwope, A., Schuecker, P., and Fassbender, R. 2005, *ApJ,* **623**, L85

Murray, S. S., et al. 2005, *ApJS,* **161**, 1

Muzzin, A., Wilson, G., Lacy, M., Yee, H. K. C., and Stanford, S. A. 2008, *ApJ,* **686**, 966

Nagai, D., Kravtsov, A. V., and Vikhlinin, A. 2007, *ApJ,* **668**, 1

Navarro, J. F., Frenk, C. S., and White, S. D. M. 1997, *ApJ,* **490**, 493

Niemack, M. D., et al. 2010, in *Society of Photo-Optical Instrumentation Engineers (SPIE) Conference Series*, Vol. 7741 of *Society of Photo-Optical Instrumentation Engineers (SPIE) Conference Series*

Paranjape, A., Gordon, C., and Hotchkiss, S. 2011, *Phys. Rev. D,* **84(2)**, 023517

Planck Collaboration, Ade, et al. 2011, *A&A,* in press (arXiv:1101.2024)

Rosati, P., et al. 2009, *A&A,* **508**, 583

Rudy, D. J., Muhleman, D. O., Berge, G. L., Jakosky, B. M., and Christensen, P. R. 1987, *Icarus,* **71**, 159

Santos, J. S., et al. 2011, *A&A,* **531**, L15

Sault, R. J., Teuben, P. J., and Wright, M. C. H. 1995, in R. A. Shaw, H. E. Payne, & J. J. E. Hayes (ed.), *Astronomical Data Analysis Software and Systems IV*, Vol. 77 of *Astronomical Society of the Pacific Conference Series*, p. 433

Stanford, S. A., et al. 2012, *ApJ,* submitted

Stanford, S. A., et al. 2005, *ApJ,* **634**, L129

Tinker, J., Kravtsov, A. V., Klypin, A., Abazajian, K., Warren, M., Yepes, G., Gottlöber, S., and Holz, D. E. 2008, *ApJ,* **688**, 709

Vanderlinde, K., et al. 2010, *ApJ* **722**, 1180

Vikhlinin, A., et al. 2009, *ApJ,* **692**, 1033

Wechsler, R. H., Bullock, J. S., Primack, J. R., Kravtsov, A. V., and Dekel, A. 2002, *ApJ,* **568**, 52

Williamson, R., et al. 2011, *ApJ,* **738**, 139